JOURNAL OF THE MECHANICAL BEHAVIOR OF BIOMEDICAL MATERIALS 39 (2014) 111–118

Available online at www.sciencedirect.com

ScienceDirect

www.elsevier.com/locate/jmbbm

Research Paper

Failure analysis of porcupine quills under axial compression reveals their mechanical response during buckling

Fernando G. Torres, Omar P. Troncoso, John Diaz, Diego Arce*

Pontificia Universidad Catolica del Peru, Dept. of Mechanical Engineering, Av. Universitaria 1801, Lima 32, Peru

ARTICLE INFO

Article history:
Received 15 May 2014
Received in revised form
27 June 2014
Accepted 17 July 2014
Available online 25 July 2014

Keywords:
Porcupine quills
Failure mechanism
Buckling
Delamination

ABSTRACT

Porcupine quills are natural structures formed by a thin walled conical shell and an inner foam core. Axial compression tests, differential scanning calorimetry (DSC), thermogravimetric analysis (TGA) and Fourier transform infrared spectroscopy (FT-IR) were all used to compare the characteristics and mechanical properties of porcupine quills with and without core. The failure mechanisms that occur during buckling were analyzed by scanning electron microscopy (SEM), and it was found that delamination buckling is mostly responsible for the decrease in the measured buckling stress of the quills with regard to predicted theoretical values. Our analysis also confirmed that the foam core works as an energy dissipater improving the mechanical response of an empty cylindrical shell, retarding the onset of buckling as well as producing a step wise decrease in force after buckling, instead of an instantaneous decrease in force typical for specimens without core. Cell collapse and cell densification in the inner foam core were identified as the key mechanisms that allow for energy absorption during buckling.

1. Introduction

Porcupines are found in two main families (about 29 species of porcupines) distributed throughout most areas in the world. They are classified as Old World porcupines and New World porcupines. Old World porcupines are found in Europe, Africa and Asia. Some examples include the North African crested porcupine *Hystrix cristata* and the African brush-tailed porcupine *Atherurus africanus*. New World porcupines are found in North, Central, and South America. These include the North American porcupine *Erethizon dorsatum* and the prehensile tailed porcupine *Coendou prehensilis*. Both families have muscles at the base of the quills enabling the quills to be raised, thereby making the animal look larger when threatened.

The *Erethizontidae* quills can be as long as 10 cm, while the *Hystricidae* quills are longer, up to 35 cm, and also have a proportionally larger diameter. All porcupine quills consist of a stiff outer sheath (cortex) and compliant porous core (medulla). The *Hystricidae* quills have additional thin solid longitudinal "stiffeners" extending radially from the cortex towards the centre of the core (Vincent and Owers, 1986; Karam and Gibson, 1994; Gibson et al., 1995).

*Corresponding author.
E-mail address: fgtorres@pucp.edu.pe (F.G. Torres).

http://dx.doi.org/10.1016/j.jmbbm.2014.07.017
1751-6161/

Quills are entirely composed of keratin. Natural keratins can be found in the outer most layer of the skin of vertebrate animals forming a protective structural covering for the organisms. Keratins are also found as fibres (hair and furs), laminates (nails, hooves, horns) and composites (quills, feathers, beaks) of mammals, birds and reptiles. This fibrous protein, known by its sulphur rich content and unique disulfide crosslinks, consists of filamentous scaffolds embedded in an amorphous matrix. Keratin materials have been categorized into α-type (α-helix) and β-type (β-sheet) based on the dominant secondary structure of the polypeptide chains. Keratin is surprisingly strong due to the S–S crosslinks and the protein's efficiency in atomic arrangement and unit cell packing (Astbury and Street, 1932; Fraser et al., 1986; Fraser and Parry, 2008).

Chou and Overfelt (2011) have studied the tensile deformation and failure of North American porcupine quills and have found that the shell of the porcupine quill is composed of 2–3 concentric layers and the quill shell exhibits a somewhat non-uniform thickness. They tested the fracture strength and the strain at fracture of North American porcupine quill at 100% RH and 65% RH and found that their tensile stiffness and strength increase as the water content decreases. In recent studies (Chou et al., 2012), it has been found that at 65% relative humidity, the mean axial elastic modulus of the shell was found to be over three times greater than the mean circumferential elastic modulus. In addition, increasing the relative humidity from 65% to 100% consistently decreased the measured values of the axial and circumferential modulus and strength and increased the fracture strain.

Vincent and Owers (1986) have measured the elastic modulus of porcupine quills. They reported an elastic modulus of 6.0 GPa for *H. cristata* quills and of 5.6 GPa for *C. prehensilis* quills. The elastic moduli reported for other keratin based structures are in the same order of magnitude as those reported for porcupine quills. For instance, Weiss, Kirchner (2010) measured the elastic modulus of the feathers from peacock's tail, and found a longitudinal elastic modulus of 3.3 GPa and a transverse modulus of 1 GPa.

Porcupine quills are one example of a thin walled conical shell structure found in nature. Other examples include plant stems, feather shafts and hedgehog spines. According to Karam and Gibson (1995a), these natural structures are typically loaded in some combination of compression and bending; failing by buckling. The interest in their study is based on the fact that cylindrical shells and tubular structures are used in several engineering applications. It has been suggested that biomimicking of such natural structures can lead to engineering structures with improved mechanical efficiency (Karam and Gibson, 1994) and to the design of efficient light structures (Van Hinte and Beukers, 1998).

In this study we have focused on porcupine quills from *C. prehensilis*, which is a porcupine from the Amazonian region belonging to the family *Erethizontidae* (New World porcupine). Axial compression tests were used to evaluate the mechanical response of the quills while attenuated total reflectance Fourier transform infrared spectroscopy (FTIR) was used to confirm the structural similarities between the inner foam and outer shell of the quills. The quill fracture morphologies were assessed with scanning electron microscopy (SEM). The main driving idea of the research presented here was to determine how the failure mechanisms that arise during axial compression of the porcupine quills affect their mechanical response and explain the differences between the predicted theoretical values of critical compressive forces and stresses with the actual measured values. Such discrepancies between predicted and experimental values had already been previously reported in the literature and further studies were needed to clarify them (Yang et al., 2013). This study aims to do that.

2. Experimental part

2.1. Materials

Porcupine quills from an Amazonian porcupine, namely, *C. prehensilis* were obtained from the city of Iquitos (Loreto, Peru). They were washed and stored in standard conditions (20 °C and 80% of relative humidity). Their dimensions were in average 1.057±0.076 mm in diameter and 20.094±0.415 mm in length.

2.2. Axial compression tests

An ESM (MARK-10) micro-mechanical testing machine was used. The tests were performed at 10 mm/min. The samples

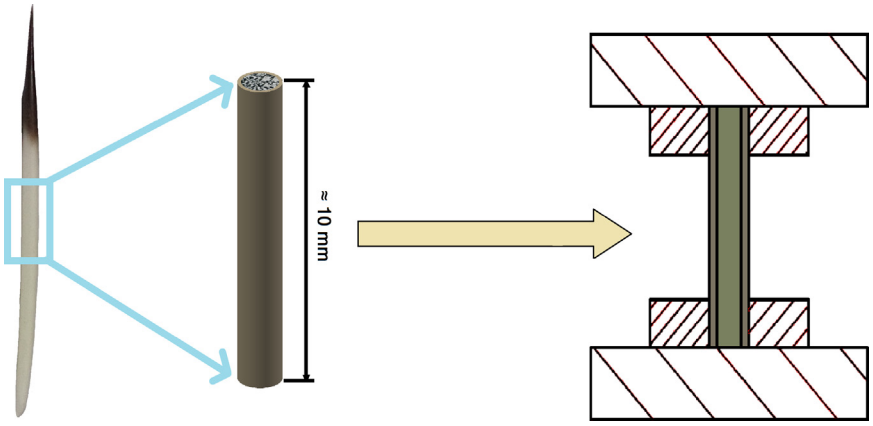

Fig. 1 – Scheme of the experimental rig used for the compression tests of porcupine quills.

were prepared in accordance with the methodology proposed by Yang et al. (2013). Briefly, the samples were cut from the central region of the quills using a surgical blade maintaining the cuts as parallel as possible to each other and perpendicular to the sides of the quill to obtain cylinders of 10 mm in length. Thin metal plates with a hole in the middle were used to fix the specimens. Both ends (top and bottom) of quill samples were positioned inside the hole of the plates and were glued with a polyacrylate adhesive as indicated in Fig. 1. In order to evaluate the effect of the foam-like core, samples were tested with core and without the core. The core was carefully removed with the aid of a needle. A minimum of 6 samples were tested for each condition.

2.3. *Scanning electron microscopy (SEM)*

The samples were cleaned with ozone before placing them into the SEM. These tests were carried out in a FEI-QUANTA 200 Scanning Electron Microscope in low vacuum with a voltage of 30 kV and a working distance in the range of 9.9–11.2 mm.

2.4. *Differential scanning calorimetry (DSC)*

DSC tests were performed in a Perkin-Elmer DSC 4000 differential scanning calorimeter. Three samples of each part of the quills were prepared: the inner part (foam), the yellow and dark outer parts (cortex). In order to prepare the samples, the quills were cut so that the foam could be removed and both inner and outer parts were cut in small pieces and loaded into sealed alumina pans. Nitrogen was used as the purging gas and the flow rate was controlled precisely at 20 ml/min. For each run, samples were heated from 25 °C to 350 °C at a heating rate of 2 °C/min.

2.5. *Fourier transform infrared spectroscopy (FTIR)*

In order to prepare porcupine quills for FTIR analysis, they were washed with distilled water then ground and dried in a desiccator. IR analysis of the samples in KBr was performed in a Lambda scientific FTIR-7600 Fourier transform spectrometer.

3. Results and discussion

Porcupine quills are thin walled conical shell structures filled with a foam-like core. Fig. 2 shows a cross section view of a representative quill. Image analysis was used to measure the characteristic dimensions of the cylindrical middle section of the sample. For the representative sample shown in Fig. 2, the cylindrical shell was around 39 μm in thickness while the average outside diameter was 1.168 mm. The foam-like core had an average cell diameter of 6.41±0.83 μm. A frequency bar graph showing the cell diameter distribution across the inner foam is given in Fig. 3.

Both, the cylindrical shell and the foam-like core are made out of keratin (Yang et al., 2013). Fig. 4 shows the FTIR spectra of the shell and core. Both spectra are similar and present the same characteristic peaks of other keratin based materials, such as amide I, amide II and amide III (Aluigi et al., 2007).

A comparison between representative DSC curves of samples of external shell and internal core of the quill is depicted in Fig. 5. These three curves present an endothermic peak in a common region of temperature (95.30–98.52 °C).

Fig. 2 – Scanning electron microscopy (SEM) image of a cross-sectional view of a porcupine quill sample showing the interior foam core surrounded by an outer shell.

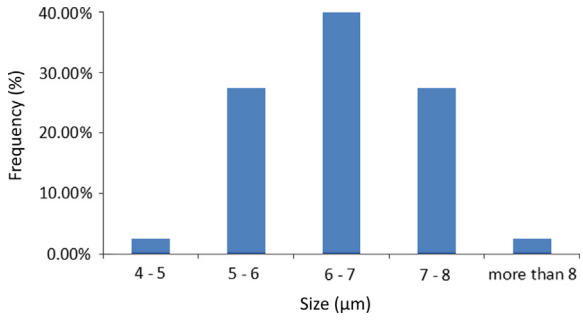

Fig. 3 – Dispersion of cell diameter of a representative sample of a porcupine core sample.

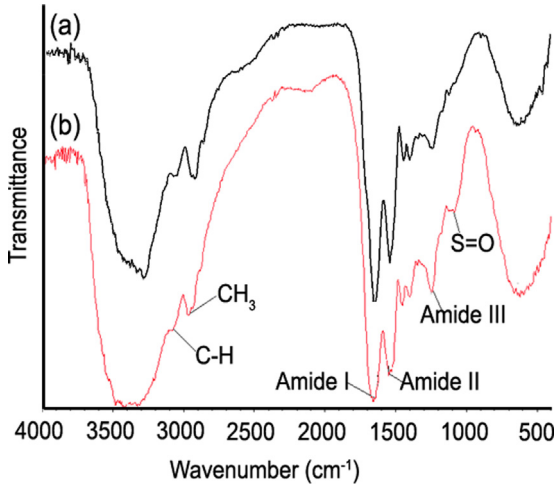

Fig. 4 – Fourier transform infrared (FTIR) spectra of the (a) internal core and the (b) external shell of a representative porcupine sample.

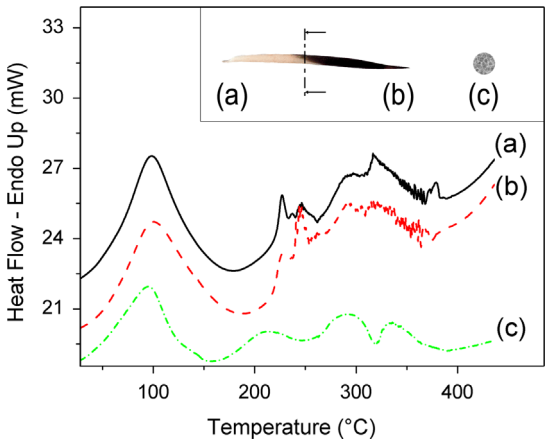

Fig. 5 – Differential scanning calorimetry (DSC) curves from samples of (a) the external yellow shell, (b) the external dark shell and the (c) internal core. (For interpretation of the references to color in this figure legend, the reader is referred to the web version of this article.)

For curve (a), at the temperature of 98.52 °C an endothermic peak is observed due to a possible loss of water, while 96.76 °C and 95.30 °C are the temperatures of endothermic peaks for curve (b) and (c), respectively. There are two more endothermic peaks for curve (c), which appear at the temperatures of around 209.18 °C and 292.21 °C. Above that temperature, the curve starts to decrease. Previous studies on keratin based materials (wool and mohair) showed that endothermic peaks at 220–230° and 230–250° can be related for the release of gaseous decomposition products, and, ultimately, to liquefaction of the organic content (Felix et al., 1963).

The analysis of the external shell (yellow and dark regions, see inset in Fig. 5) of the quill has shown that both curves (a) and (b) have a similar behaviour. At temperatures of 226.98 °C for yellow region (b) and 227.85 °C for dark region (c) a similar peak is observed, which correspond to the temperatures of denaturation of crystals of α-keratin with different molecular weights (Monterio et al., 2005). Different endothermic peaks observed at a temperature higher than 260 °C are probably due to denaturation of crystalline fraction with different molecular weight.

From these thermal and IR spectroscopy studies it is possible to confirm that both shell and core are made out of the same type of keratin based material and display similar physical properties.

As expected, axial compression tests showed that the quills used in this study failed by buckling. In order to calculate the stress values we considered the cross section area of the quill sheath, neglecting the influence of the foam core, as in Vincent and Owers (1986). Fig. 6a depicts a representative stress–strain curve of a sample with foam core and Fig. 6b shows the stress–strain curve of a sample without the core. The compressive stress–strain curves presented here are in agreement with previous studies of porcupine quills from other species (Yang et al., 2013).

It is worth noting that the tests presented here account for the behaviour of the middle (cylindrical) section of the quills. Porcupine quills are really conical and display some degree of

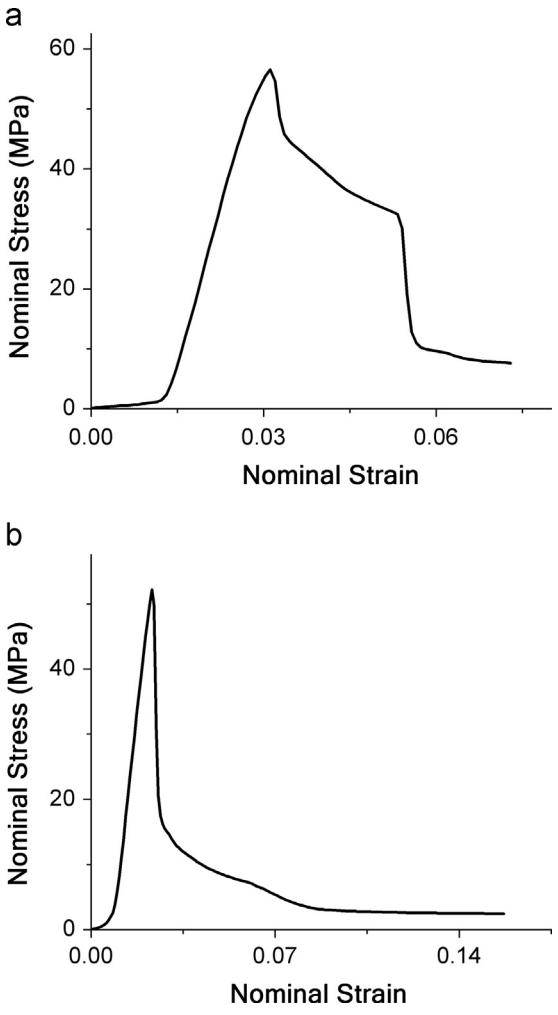

Fig. 6 – Stress–strain representative curves of porcupine quills samples: (a) quills with core and (b) quills without core.

Table 1 – Mechanical parameters from compressive tests of quills with foam (1) and without foam (2).

Type of sample	σ (MPa)	ε_R (%)	$E_{1-3\%}$ (GPa)
With core	52.5±10.0	2.8±0.4	1.8±0.1
Without core	58.1±18.2	2.4±0.3	1.8±0.1

curvature along their axis. It is reasonable to expect that the length of the quills and their initial curvature affects the value of the critical buckling stress. For instance, when Vincent and Owers (1986) tested quills extracted from *Hystrix* porcupines, they used the whole quills for axial compression tests and found a critical buckling stress of 0.7 MPa. By contrast, Yang et al. (2013) also used quills from *Hystrix* porcupines but they only tested the middle section of the quills. The critical buckling stress they measured was 167.9 MPa.

Table 1 shows the buckling stress, the strain at buckling and the Young's modulus of the samples studied. The mean buckling stress obtained for samples with and without foam were 52.5±10.0 MPa and 58.1±18.2 MPa, respectively. These

values are also in agreement with the values reported by Yang et al. (2013) for *Erethizon* quills. It can be observed that the buckling stress of samples without core showed a much larger scatter than the values found for samples with core. The higher standard deviation in the results of samples without core could be due to damage produced in the preparation of the samples when the foam core was removed with the aid of a needle.

Yang et al. (2013) have investigated the structure and compressive properties of quills from *Hystrix* and *Erethizon* porcupines. They have found that the mean local buckling strength of *Erethizon* and *Hystrix* quills is 61.3 MPa and 167.9 MPa, respectively. Timoshenko and Gere (1961) have calculated the critical stress (σ_0) at which buckling takes place for a thin walled, hollow, cylindrical shell according to:

$$\sigma_0 = \frac{E \times t}{a \times \sqrt{3 \times (1-\nu^2)}} \quad (1)$$

where a: radius of cylinder, t: thickness of cylinder, E: Young's modulus, ν: Poisson's ratio

In order to model the mechanical behaviour of a cylindrical shell with a compliant elastic core (σ_{cr}), Karam and Gibson (1995a) have proposed the following equation:

$$\sigma_{cr} = \sqrt{3 \times (1-\nu^2)} \times \sigma_0 \times f_1 \quad (2)$$

where σ_0 is the critical stress for a quill without core (Eq. (1)) and f_1 is calculated by using Eq. (3)

$$f_1 = \frac{1}{12 \times (1-\nu^2)} \times \frac{a/t}{(\lambda_{cr}/t)^2} + \frac{(\lambda_{cr}/t)^2}{a/t} + \frac{2 \times \alpha}{(3-\nu_c) \times (1+\nu_c)} \times (\lambda_{cr}/t) \times (a/t) \quad (3)$$

here α is the relation between the Young's moduli ($\alpha = E_c/E$) and λ_{cr} is the half buckling wavelength divided by π. The relation between λ_{cr} and the thickness t is obtained by:

$$\frac{\lambda_{cr}}{t} = \left[\frac{(3-\nu_c) \times (1+\nu_c)}{12 \times (1-\nu^2)}\right]^{1/2} \times \left(\frac{E}{E_c}\right)^{1/2} \quad (4)$$

The analysis of Karam and Gibson (1995a) provides the critical strength and load when the Young's moduli and Poisson's ratios of both shell and core, as well as the radius and thickness of the shell are known.

Vincent and Owers (1986) have reported the modification of the Euler equation of buckling in order to include the effect of the quills' curvature. For the analysis of the data presented here, the quills were considered to be straight (specimens were extracted from the middle portion of the quills) and the effect of curvature was neglected.

Eqs. (1) and (2) have been used to compare the experimental values obtained with the theoretical predictions. The experimental Young's modulus measured from the compression tests was used as the cortex Young's modulus (E) in Eq. (1). For the core modulus (E_c) we used a value derived from $E_c/E = 0.014$ (Yang et al., 2013). The geometrical dimensions (a and t) were measured from each sample before testing. The Poisson's modulus used was the same for both cortex and core, $\upsilon = \upsilon_c = 0.3$ (Yang et al., 2013).

In both cases, for hollow quills and for filled quills, the predicted theoretical values were higher than the measured values.

In the case of hollow quills, the average theoretical buckling stress calculated was 74.2±12.4 MPa while the experimentally measured value was 58.1±18.2 MPa. For filled quills, the theoretical value calculated was 128.8±23.9 MPa while the experimental value was 52.5±10.0 MPa. The standard deviation of the theoretical values accounts for the geometrical characteristics of each sample.

Such discrepancy between theoretical and experimental values has also been reported by Yang et al. (2013). They carried out compressive axial tests for quills from two different species of porcupines, *Hystrix* and *Erethizon*. According to their calculations and experiments, the theoretical buckling stress of *Hystrix* quills was higher than the experimental values. By contrast, for *Erethizon* quills, the theoretical values were lower than the experimental values.

3.1. *Failure analysis*

For engineering structures, it has been claimed that in practice, the measured elastic buckling stress values are always lower than theoretical values. Some authors have suggested that this is due to unavoidable geometric and materials defects that cause premature loss of stability. In engineering design, safety factors reduce the theoretical value of the critical buckling load down to 30–40% of the original value (Kollár and Dulácska, 1984). For porcupine quills, Yang et al. (2013) claimed that these differences could be due to the cortex effect, non-uniform foam cell sizes, non-uniform cell wall thickness and to the assumption that the density of the cell walls and stiffeners are the same as that of solid keratin. Moreover, the formulas used for predicting the theoretical values consider that the quills were straight at the beginning of the experiment, but the all the samples tested were slightly curved from the start.

For the present study, SEM tests were carried out in order to analyze the failure zone of the buckled samples. Fig. 7a–c, shows the external part of a representative quill after buckling has taken place during the compression tests. The damage is readily appreciated and occurred in the middle part of the quill. Several cracks with varying dimensions can be observed on the cortex surface. The cracks seem to grow across the cortex thickness, in a direction perpendicular to the micrograph plane. On the other hand, Fig. 8 shows a longitudinal cross section of a buckled sample. Arrows indicate zones were delamination has occurred. It is reasonable to expect that the type of delamination observed in Fig. 8 decreases the resistance of the quill to compressive stress.

In the case of laminated composites materials, delamination buckling is a mechanism that affects the buckling resistance of structures. It has been suggested that laminated composites present delamination zones in their original structure that are more likely to be affected when an external load is applied (Kachanov, 1988). When delamination buckling takes place in a laminated composite material, the structure will fail by buckling at a stress lower that the theoretical critical buckling stress.

Using a reverse engineering approach, we have calculated the values of the critical stress for the delamination zones before buckling based on the analysis of Kachanov (1988). According to Kachanov, local delamination of laminated

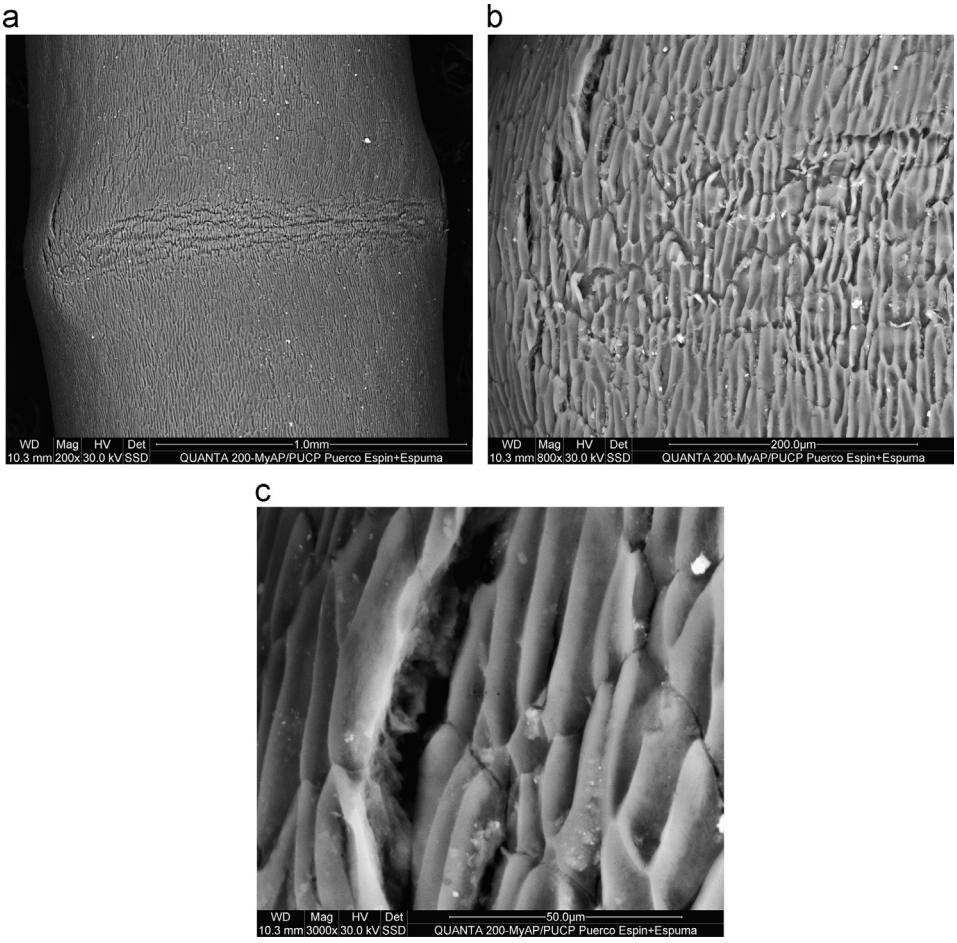

Fig. 7 – Scanning electron microscopy (SEM) images of the external shell at (a) 200 × magnification, (b) 800 × magnification and (c) 3000 × magnification.

composites usually takes place at the surface layer and can be modelled as the case of buckling of a strip with fixed ends. For this case (when $\varepsilon_z=0$), the Euler buckling equation takes the following form:

$$\sigma_c = \frac{\pi \times E}{3 \times (1-\nu^2)} \times \left(\frac{h}{l}\right)^2 \quad (5)$$

where E is the Young's Modulus, υ is the Poisson ratio, h is the length of the delamination zone and l is the thickness of the layer between the delamination zone and the surface. Eq. (5) was used to calculate the critical stress due to delamination in 20 different delaminated zones (Table 2).

Fig. 9 shows the probability of failure for different values of stress due to delamination buckling. The probability of failure calculated using a Weibull distribution indicates that the characteristic critical stress due to delamination buckling was 47.36 MPa (when $\ln(\ln(1/1-F))=0$). This value is in agreement with the experimental critical stress value obtained (52.5 ± 10.0 MPa). This suggests that delamination buckling determines the critical stress rather than the Euler-ian critical buckling stress calculated with the previous equations (Eqs. (1)–(4)).

Fig. 8 also shows that the foam-like core is affected by buckling. Cell collapse and densification can be identified as the main failure mechanisms of the inner foam structure. The

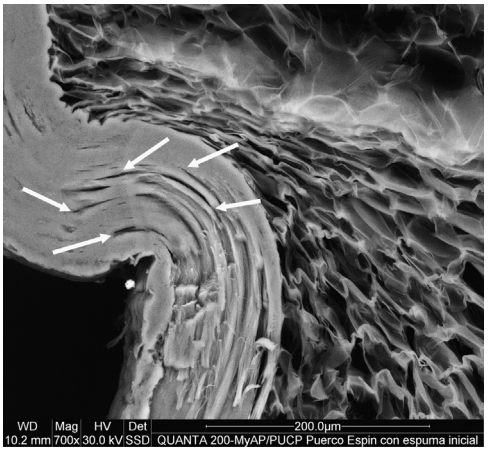

Fig. 8 – Scanning electron microscopy (SEM) image of longitudinal cross section of a representative buckled sample. Arrows indicates zones were delamination buckling occurs.

influence of the core on the buckling resistance of quills has been studied in the past. Karam and Gibson (1995b) have calculated the critical buckling load of several natural structures formed by cylindrical shells with foam-like cores. They have compared the critical buckling load of such structures with core

Table 2 – Critical buckling stress of delamination zones.

Samples	E (GPa)	υ	l (mm)	h (mm)	σc (GPa)
1	1.7	0.3	0.122	0.009	0.0334
2	1.7	0.3	0.070	0.010	0.1254
3	1.7	0.3	0.051	0.008	0.1512
4	1.7	0.3	0.071	0.010	0.1219
5	1.7	0.3	0.018	0.008	1.2140
6	1.7	0.3	0.035	0.010	0.5017
7	1.7	0.3	0.037	0.008	0.2873
8	1.7	0.3	0.070	0.013	0.2120
9	1.7	0.3	0.033	0.007	0.2765
10	1.7	0.3	0.035	0.011	0.6071
11	1.7	0.3	0.090	0.021	0.335
12	1.7	0.3	0.077	0.023	0.548
13	1.7	0.3	0.053	0.026	1.479
14	1.7	0.3	0.489	0.027	0.019
15	1.7	0.3	0.063	0.023	0.819
16	1.7	0.3	0.041	0.009	0.296
17	1.7	0.3	0.083	0.009	0.072
18	1.7	0.3	0.028	0.008	0.502
19	1.7	0.3	0.029	0.008	0.468
20	1.7	0.3	0.048	0.009	0.216

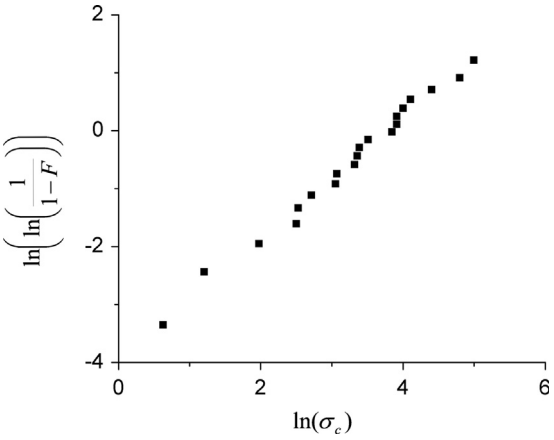

Fig. 9 – Weibull diagram of critical buckling stress of a quill determined for delamination buckling.

and without core. For stem plants they suggested that buckling resistance of pure axial compression is higher without core. In the case of porcupine quills, they have found that the critical buckling strength can be higher with core for some species and lower for other species. By contrast, pure bending tests showed that the foam-like core effectively increase the bending resistance of porcupine quills. The buckling strength of porcupine quills with core is higher than the buckling stress of porcupine quills without core.

3.2. *Analysis of the foam core function*

From an engineering point of view, it could be expected that the foam core should work as an energy dissipating medium if we consider a porcupine quill as a composite structure. In engineering structures this is usually achieved by increasing the critical strain of the material during deformation or by changing its load-deformation behaviour after buckling occurs. In order to clarify the function of the foam core of porcupine quills, we have calculated the mean critical strains for specimens with and without core and found that these were 2.8±0.4% and 2.4±0.3% for quills with core and without core, respectively.

From the stress–strain curves we calculated the areas under the curves in order to obtain the energy dissipated during the compression tests. The results show that for the representative curves presented in Fig. 6a and b, the quills with core absorbed 67.8% more energy than their counterparts without core. The average value of the increment in absorbed energy was 61.30%±8.9%

This increase in energy dissipation can be confirmed if we analyze the force versus time curves from the compression tests presented earlier, which are given in Fig. 10. As can be observed from Fig. 10, for a quill with core, the onset of buckling is retarded with regard to the specimen without core. But more importantly, a dramatic decrease in force can be observed after the onset of buckling for the quill without core, whereas for the specimen with core a stepwise decrease in force is observed. This gradual decrease in force should be associated to cell collapse and cell densification as observed in Fig. 8.

Fig. 10 shows the stress–time curves obtain from compression test of porcupine quills with core (a) and porcupine quills without core (b). We can appreciate that quills with core takes more time before buckling. Also we determined the average values of critical time for the tested quills before buckling and the values we obtain were 3.6±0.8 s and 2.9±0.4 s for samples with and without core respectively, having a 24.8% of difference between each other.

4. Conclusions

We have studied the mechanical response of porcupine quills under pure axial compression. The predicted theoretical values for the critical buckling stress of the quills, calculated following Karam and Gibson (1995a) approaches produced higher values than the experimental values recorded in the

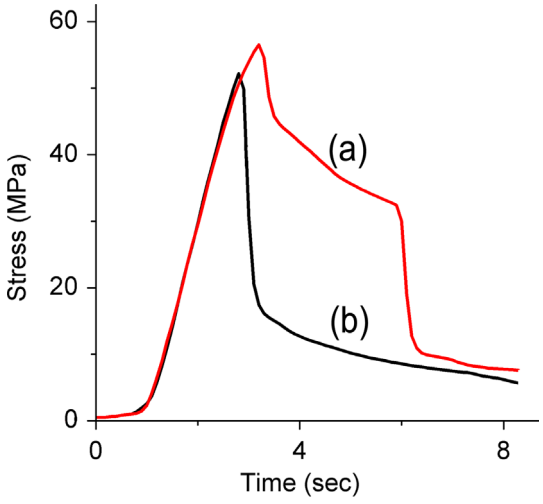

Fig. 10 – Stress–time curves of porcupine quills samples: (a) quills with core and (b) quills without core.

experiments described here. These discrepancies were clarified by analyzing the failure mechanisms in the compressed specimens. The failure mechanisms that occur during buckling were analyzed by scanning electron microscopy (SEM), and it was found that delamination buckling is mostly responsible for the decrease in the measured buckling stress of the quills with regard to predicted theoretical values.

Our analysis also confirmed that the foam core works as an energy dissipater improving the mechanical response of an empty cylindrical shell, retarding the onset of buckling as well as producing a step wise decrease in force after buckling, instead of an instantaneous decrease in force typical for specimens without core. This step wise decrease in energy, which is also observed for fibre reinforced composite materials, can be, in the case of porcupine quills, associated to cell collapse and densification mechanisms in the inner core, which were also confirmed by scanning electron microscopy. These results suggest that the effect of the core on energy dissipation can be observed after the onset of buckling. The foam core would probably retard the catastrophic failure of the quills after buckling has taken place.

Based on our results and conclusions, we believe that the development of bioinspired materials based on the quill basic structure should consider the analysis of the failure mechanisms that occur when subjected to specific loading conditions.

Acknowledgements

The authors would like to thank the Peruvian Science and Technology Program (FINCyT-Peru) and the Vice-Rectorate for Research of the Pontificia Universidad Catolica del Peru (VRI-PUCP) for their financial support.

REFERENCES

Aluigi, A., Zoccola, M., Vineis, C., Tonin, C., Ferrero, F., Canetti, M., 2007. Study on the structure and properties of wool keratin regenerated from formic acid. Int. J. Biol. Macromol. 41, 266–273.

Astbury, W.T., Street, A., 1932. X-ray studies of the structure of hair, wool, and related fibres. I—General. Philos. Trans. R. Soc. London, Ser. A 230, 75–101.

Chou, S.F., Overfelt, R.A., 2011. Tensile deformation and failure of North American porcupine quills. Mater. Sci. Eng., C 31, 1729–1736.

Chou, S.F., Overfelt, R.A., Miller, M.E., 2012. Anisotropic mechanical behaviour of keratin tissue from quill shells of North American porcupine (*Erethizon dorsatum*). Mater. Sci. Eng., A 557, 36–44.

Felix, W.D., McDowall, M.A., Eyrring, H., 1963. The differential thermal analysis of natural and modified wool and mohair. Text. Res. J. 33, 465–471.

Fraser, R.D., MacRae, T.P., Parry, D.A., Suzuki, E., 1986. Intermediate filaments in alpha-keratins. Proc. Nat. Acad. Sci. U.S.A. 83, 1179–1183.

Fraser, R.D., Parry, D.A., 2008. Molecular packing in the feather keratin filament. J. Struct. Biol. 162, 1–13.

Gibson, L.J., Ashby, M.F., Karam, G.N., Wegst, U., Shercliff, H.R., 1995. The mechanical properties of natural materials. II. Microstructures for mechanical efficiency. Proc. R. Soc. London, Ser. A 450, 141–162.

Kachanov, L.M., 1988. Delamination Buckling of Composite Materials, first ed. Kluwer Academic Publishers, The Netherlands.

Karam, G.N., Gibson, L.J., 1994. Biomimicking of animal quills and plant stems: natural cylindrical shells with foam cores. Mater. Sci. Eng., C 2, 113–132.

Karam, G.N., Gibson, L.J., 1995a. Elastic buckling of cylindrical shells with elastic cores—I. Analysis. Int. J. Solids Struct. 32, 1259–1283.

Karam, G.N., Gibson, L.J., 1995b. Elastic buckling of cylindrical shells with elastic cores—II. Experiments. Int. J. Solids Struct. 32, 1285–1306.

Kollár, L., Dulácska, E., 1984. Buckling of Shells for Engineering, first ed. Wiley, New York.

Monterio, V.F., Maciel, A.P., Longo, E., 2005. Thermal analysis of caucasian human hair. J. Therm. Anal. Calorim. 79, 289–293.

Timoshenko, S.P., Gere, J.M., 1961. Theory of Elastic Stability, second ed. MacGraw-Hill, New York.

Van Hinte, E., Beukers, A., 1998. Lightness: The Inevitable Renaissance of Minimum Energy Structures, cero ed. 010 Uitgeverij.

Vincent, J.F.V., Owers, P., 1986. Mechanical design of hedgehog spines and porcupine quills. J. Zool. 210, 55–75.

Weiss, I.M., Kirchner, H.O.K., 2010. The peacock's train (*Pavo cristatus* and *Pavo cristatus mut. alba*) I. structure, mechanics, and chemistry of the tail feather coverts. J. Exp. Zool. A 313, 690–703.

Yang, W., Chao, C., McKittrick, J., 2013. Axial compression of a hollow cylinder filled with foam: a study of porcupine quills. Acta Biomater. 9, 5297–5304.